

Ionization potential and excitation energy calculations for Ba⁺ using the relativistic coupled-cluster method

Geetha Gopakumar, Holger Merlitz, Sonjoy Majumder, Rajat K. Chaudhuri, and B. P. Das
 Non-Accelerator Particle Physics Group, Indian Institute of Astrophysics, Bangalore 560 034, India

Uttam Sinha Mahapatra and Debashis Mukherjee
 Indian Association for Cultivation of Science, Calcutta 700 032, India

(Received 3 March 2001; published 13 August 2001)

We report the results of our relativistic coupled cluster singles, doubles, and partial triples calculations of the ionization potentials (IP) and excitation energies (EE) for different low-lying levels of Ba⁺. The accuracies of the IP's and EE's are approximately 0.2% and 1%, respectively. The inclusion of the triple excitations were crucial to achieve this degree of precision.

DOI: 10.1103/PhysRevA.64.032502

PACS number(s): 31.15.Dv, 31.50.Df, 32.10.Hq

It is now well known that atomic parity nonconservation (PNC) has the potential to probe physics beyond the standard model [1]. The atom that is currently best suited for this purpose is cesium for which the combined accuracy of PNC experiment and theory is below 1% [2]. However, there are other promising proposals to observe PNC in atomic systems. One of these involves applying the techniques of ion trapping and laser cooling to Ba⁺ [3]. It has been pointed out that certain transitions in Ba⁺ and Ra⁺ could yield unambiguous information about nuclear-spin dependent PNC [4]. Unlike the $S \rightarrow S$ transition for cesium, the transitions of interest for Ba⁺ are $S \rightarrow D$. The PNC calculations on Ba⁺ are more demanding than those on cesium, as a many-body description of the D states, unlike the S states, requires configurations that are relatively complex. While there have been attempts to calculate PNC amplitudes in Ba⁺ [4,5], further work, based on rigorous many-body approaches, is needed. The electric dipole transition amplitude induced by the short-range electron-nucleon PNC interaction, is sensitive to the region close to as well as far away from the nucleus. It is therefore necessary to perform calculations of a variety of atomic properties to estimate the accuracy of the PNC calculations. This paper, where the results of our high-precision calculations of ionization potential (IP) and excitation energy (EE) for various states of Ba⁺ based on the relativistic non-linear coupled cluster singles, doubles, and partial triples [CCSD(T)] method are presented, represents the first step in this direction.

The IP of the valence electron is given by

$$V_i = \langle \Psi^N | H | \Psi^N \rangle - \langle \Psi^{N-1} | H | \Psi^{N-1} \rangle, \quad (1)$$

where $|\Psi^{N-1}\rangle$, $|\Psi^N\rangle$ represent states of the $N-1$ and N electron systems, respectively, and H is the exact no-virtual pair Dirac-Coulomb Hamiltonian of the system as discussed by Refs. [6,7], which can be expanded as

$$H = \sum_i T_i + \sum_{i < j} v_{ij}. \quad (2)$$

The matrix elements of T and v are given by

$$\langle i | T | j \rangle = \int \phi_i^*(1) T_1 \phi_j(1) d\tau_1 \quad (3)$$

and

$$\langle ij | v | kl \rangle = \int \int \phi_i^*(2) \phi_j^*(2) v_{12} \phi_k(1) \phi_l(1) d\tau_1 d\tau_2, \quad (4)$$

where

$$T_i = c \alpha_i p_i + c^2 (\beta_i - 1) + V_{nuc}(i) \quad (5)$$

and

$$v_{ij} = \frac{1}{r_{ij}}. \quad (6)$$

Effects due to Breit, negative-energy states, and radiation corrections are omitted, since the property we are interested in, for present paper, has a negligible effect due to them. We have used CCSD(T) with the even-parity channel approximation [8] to go beyond the DF approximation. The selection rules and the angular momentum reduction techniques are explained in the earlier paper [9]. The code is parallelized using message passing interface and the details will be reported in another paper.

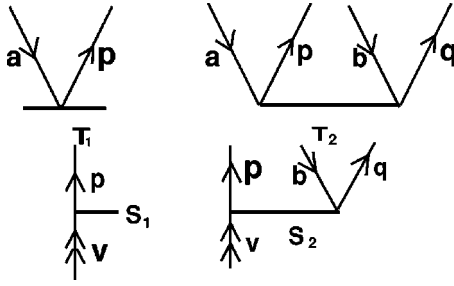
In our coupled cluster calculations, we use the DF reference state corresponding to a $(N-1)$ -electron closed-shell configuration, then add one electron to the k th virtual orbital and obtain the N -electron system on which calculations are carried out. The addition of an electron to the k th virtual orbital to the reference state, can therefore be written as

$$|\Phi_k^N\rangle = a_k^\dagger |\Phi_0\rangle. \quad (7)$$

Any general state can be written in open-shell coupled-cluster model (CCM) [10] as

$$|\Psi_k\rangle = \{e^{S_k}\} e^T |\Phi_k\rangle, \quad (8)$$

where $|\Phi_k\rangle$ is the DF reference state for an open-shell configuration with T and S operators defined as


 FIG. 1. Diagrammatic representation of T and S operators.

$$T = T_1 + T_2 = \sum_{ap} a_p^+ a_a t_a^p + \sum_{abpq} a_p^+ a_q^+ a_b a_a t_a^{pq} \quad (9)$$

and

$$S_k = S_{k1} + S_{k2} = \sum_p a_p^+ a_k s_k^p + \sum_{pqa} a_p^+ a_q^+ a_a a_k s_{ka}^{pq} \quad (10)$$

Here T represents the operator that produces excitations from the core and S the excitation from valence and valence-core interactions. In our notation, a, b, \dots denote core orbitals and p, q, r, \dots denote virtual orbitals. Therefore T acts on the $N-1$ electron system and both T and S act on the N electron system. Diagrammatically these operators are given in Fig. 1.

For the nonlinear case, the terms that give connected diagrams are $T_1 T_1$, $T_1 T_2$, $T_2 T_2$, $T_1 T_1 T_1$, $T_1 T_1 T_2$, and $T_1 T_1 T_1 T_1$. For the present calculation we have taken only the terms $T_2 T_2$, $T_1 T_2$, and $T_1 T_1$ to reduce the computation time for the evaluation of the T amplitudes. This approximation is justified since the T_1 cluster amplitudes are small. Typical diagrams that contribute to the nonlinear cluster amplitudes are given in Fig. 2. For the open shell calculation, we have included approximate triples, which arise via the VT_2 and VS_2 channels in the IP calculations obtained using single and double excitations. Typical diagrams, which contribute to such an effect, are given in Fig. 3.

We consider first the $N-1$ electron closed shell. The equation for this system is given by

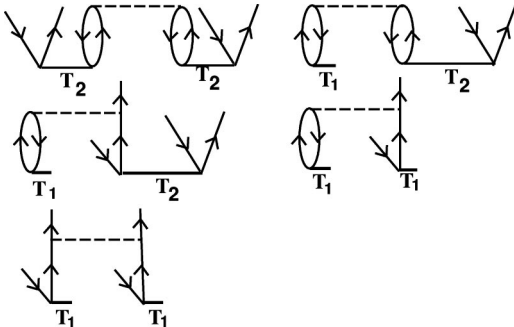
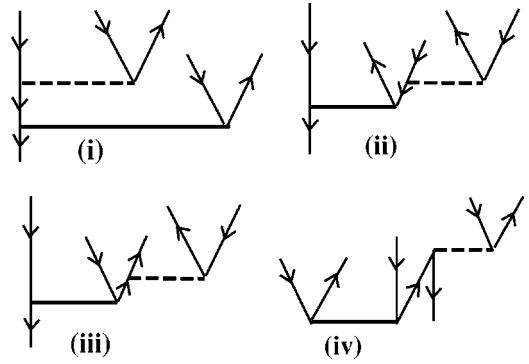


FIG. 2. Typical diagrams representing the nonlinear terms.


 FIG. 3. Typical diagrams representing the approximate triples diagrams: (i), (ii), and (iii) give the VS_2 contributions, and (iv) gives the VT_2 contributions.

$$H|\Psi^{N-1}\rangle = E^{N-1}|\Psi^{N-1}\rangle. \quad (11)$$

By suitable substitutions using the T operator we obtain two equations. One of them gives the coupled cluster amplitudes and the other the correlation energy. The equation to determine the correlation energy is

$$\Delta E^{N-1} = \langle \Phi_0 | \bar{H}_N | \Phi_0 \rangle \quad (12)$$

and the equation for the coupled cluster amplitudes is obtained by projecting on singly and doubly excited determinants, which reduces to

$$\langle \Phi^* | \bar{H}_N | \Phi_0 \rangle = 0, \quad (13)$$

where $H_N = H - \langle \Phi_0 | H | \Phi_0 \rangle$ and $\bar{H}_N = e^{-T} H_N e^T$.

We turn next to the N electron system, which satisfies the equation

$$H|\Psi_k^N\rangle = E_k^N|\Psi_k^N\rangle. \quad (14)$$

Carrying out mathematical operations similar to those used earlier involving the T and S operators, we obtain an equation for the IP and another one for the coupled-cluster amplitudes. The equation for the evaluation of the ionization potential is

$$\Delta E_k^N = \langle \Phi_k^N | \bar{H}_N (1 + S_k) | \Phi_k^N \rangle \quad (15)$$

and the equation for the coupled cluster amplitudes is obtained similarly by projecting on the singly and doubly excited determinants, which leads to

$$\langle \Phi_k^{*,N} | \bar{H}_N S_k | \Phi_k^N \rangle = \Delta E_k^N \langle \Phi_k^{*,N} | S_k | \Phi_k^N \rangle - \langle \Phi_k^{*,N} | \bar{H}_N | \Phi_k^N \rangle. \quad (16)$$

Here we first solve for ΔE_k^N using Eq. (15) and then solve Eq. (16) to get new S amplitudes, which we use in turn to get new ΔE_k^N till self-consistency is achieved. Here ΔE_k^N is the

TABLE I. Number of Gaussian basis functions used for the computation of orbitals of each symmetry for Ba⁺.

<i>s</i> (1/2)	<i>p</i> (1/2)	<i>p</i> (3/2)	<i>d</i> (3/2)	<i>d</i> (5/2)	<i>f</i> (5/2)	<i>f</i> (7/2)	<i>g</i> (7/2)	<i>g</i> (9/2)	<i>h</i> (9/2)	<i>h</i> (11/2)
32	28	28	25	25	20	20	15	15	10	10

difference in energy between the closed-shell state Ψ^{N-1} and the open-shell state Ψ_k^N and in comparison with Eq. (1), IP is the negative of ΔE_k^N . The next step in the calculation is the inclusion of the triple excitations in an approximate way shown below:

$$S_{abk}^{pqr} = \frac{\widehat{VT}_2 + \widehat{VS}_2}{\epsilon_a + \epsilon_b + \epsilon_k - \epsilon_p - \epsilon_q - \epsilon_r}, \quad (17)$$

where S_{abk}^{pqr} are the amplitudes corresponding to the simultaneous excitation of orbitals a, b, k to p, q, r , \widehat{VS} is the contraction of all creation annihilation operators, and ϵ_i orbital energy of the i th orbital. This contribution is added to the energy obtained using singles and doubles. Once the IP's are computed, the EE's are obtained by finding the difference between the IPs of the valence (6*s*) and appropriate virtual orbitals.

The single-particle orbitals used in our calculations, are part numerical and part analytical. The underlying idea of this new hybrid approach is to represent the core, valence, and a certain number of bound virtual orbitals by numerical solutions of the DF equation, and the remaining virtual orbitals are expressed as linear combinations of kinetically balanced Gaussian type orbitals (GTO's) [11]. The GTO's are of the form

$$G_{i,k}(r) = r^k e^{-\alpha_i r^2}, \quad (18)$$

where $k=0,1,\dots$ for s, p, \dots functions. We have used the even tempering condition

$$\alpha_i = \alpha_{i-1} \beta, \quad i = 1, \dots, N, \quad (19)$$

where N is the number of basis functions for a given symmetry, and α_0 and β are parameters required to describe the GTO's.

The starting point of our calculation is the generation of DF orbitals for the Ba⁺⁺ core. These orbitals are expressed as linear combinations of GTO's on a grid and the DF matrix is diagonalized to yield the occupied and virtual orbitals [12]. The parameters N , α_0 , and β are adjusted to get the bound orbitals as close to the numerical orbitals as possible [13–15]. We have used $\alpha_0 = 0.00725$ and $\beta = 2.73$ for the present calculation. The number of GTO's used in our calculation for orbitals of different symmetries is given in Table I. We take the core and some of the low-lying virtual orbitals as numerical orbitals generated from the GRASP multiconfiguration Dirac Fock [16] package. These orbitals are then made orthogonal with the rest of the Gaussian virtual orbitals through the Schmidt orthogonalization procedure, and the orthogonalized orbitals in turn are used for expanding the virtual orbitals. The DF Hamiltonian is then diagonalized only in this virtual space to get the complete basis. The advantage of this method over the one we had used earlier [12], is the freedom one has in choosing the orbitals. For example, in the present approach, one cannot only represent the core, but also an appropriate number of unoccupied single-particle states by numerical bound orbitals. The details of this new method for orbital generation will be reported in a forthcoming paper.

For the coupled cluster calculations, we have restricted the basis by imposing lower and upper bounds in energy for all the single-particle orbitals as -100 and 100 a.u. for all the symmetries except h . This was done to reduce the huge memory requirement, which is needed in storing the matrix

TABLE II. Orbital generation.

Symmetry	No of orbitals in each symmetry	Numerical orbitals used in the calculation	Gaussian orbitals used in calculation
<i>s</i>	9	3,4...8 <i>s</i>	9 <i>s</i> ,...11 <i>s</i>
<i>p</i> (1/2)	9	3 <i>p</i> ,...8 <i>p</i>	9 <i>p</i> ,...11 <i>p</i>
<i>p</i> (3/2)	9	3 <i>p</i> ,...8 <i>p</i>	9 <i>p</i> ,...11 <i>p</i>
<i>d</i> (3/2)	10	3 <i>d</i> ,...7 <i>d</i>	8 <i>d</i> ,...12 <i>d</i>
<i>d</i> (5/2)	10	3 <i>d</i> ,...7 <i>d</i>	8 <i>d</i> ,...12 <i>d</i>
<i>f</i> (5/2)	9	4 <i>f</i> ,5 <i>f</i>	6 <i>f</i> ,...12 <i>f</i>
<i>f</i> (7/2)	9	4 <i>f</i> ,5 <i>f</i>	6 <i>f</i> ,...12 <i>f</i>
<i>g</i> (7/2)	9		5 <i>g</i> ,...13 <i>g</i>
<i>g</i> (9/2)	9		5 <i>g</i> ,...13 <i>g</i>
<i>h</i> (9/2)	7		6 <i>h</i> ,...12 <i>h</i>
<i>h</i> (11/2)	7		6 <i>h</i> ,...12 <i>h</i>

TABLE III. Nonlinear CCSD values for IP's in units of (a.u.) (in parentheses: contribution from partial triples)

Orbital	Experiment	Present	Eliav <i>et al.</i> [17]	Guet and Johnson [18]
$6s(1/2)$	0.367 64	0.368 14 (-0.0130784)	0.368 48	0.373 08
$5d(3/2)$	0.345 43	0.346 23 (-0.019412)	0.344 48	0.351 72
$5d(5/2)$	0.341 78	0.342 11 (-0.018676)	0.340 72	0.347 48
$6p(1/2)$	0.275 34	0.275 68 (-0.010146)	0.275 55	0.277 42
$6p(3/2)$	0.267 62	0.267 81 (-0.009801)	0.267 77	0.269 46

elements of the dressed operator \bar{H}_N and the two electron Coulomb interaction in the fast memory. We consider excitations from the $n=3$ shell and above. Considering excitations from $n=1$ and above with a 7 symmetry calculation, the IP value obtained for $6s$ is around $-0.368\,615\,99$, which in comparison with $n=2$ and above, is $-0.368\,6409$. This establishes that the contribution due to omitted shells less than 3 to be 0.01% to IP's. It is clear from calculations by Kaldor *et al.* [17] that high-lying virtual orbitals contribute very little to the excitation energies. Since the basis that we have used is fairly large with the core and the low-lying virtuals as numerical orbitals, the error arising from the basis will be less than 0.1%. Numerical orbitals used in the above calculation with respect to each symmetry, are given in Table II. Here we have calculated the IP's of low-lying levels given by $6s_{1/2}$, $5d_{3/2,5/2}$, and $6p_{1/2,3/2}$. The EE's are essential for the calculation of the lifetimes of the levels, where the $5d$ orbitals connect to $6s$ orbital through $E2$ transition and $6p$ orbital through $E1$ transition.

The total number of T amplitudes for the above calculation is 233 988. The linear CCSD converged within 4 cycles with a self-consistency of 10^{-7} , with a total CPU time of 35 h. The nonlinear part of the code took 3 iterations, with each iteration taking on an average 64 h. Using the T amplitudes, the dressed Hamiltonian matrix and the IP's of different orbitals, were computed. In comparison with the T amplitude calculation, the computation time for the S amplitudes is about an order of magnitude smaller. In addition, the dressed Hamiltonian and the Coulomb matrix elements were stored in random access memory (RAM), which considerably speeded up the calculations.

The values of the correlation energy obtained using second-order many-body perturbation theory (MBPT), linear, and nonlinear CCSD, are given below:

$$\Delta E^{N-1} \text{ (second order MBPT)} = -1.94 \text{ a.u.}$$

$$\Delta E^{N-1} \text{ (linear CCSD)} = -1.83 \text{ a.u.}$$

$$\Delta E^{N-1} \text{ (nonlinear CCSD)} = -1.82 \text{ a.u.}$$

From the above data, it can be inferred that the nonlinear contribution is 0.6% of the total correlation energy. The results of the calculations of our IP's and EE's are given in Table III and Table IV and compared with the previous calculations by Guet and Johnson [18] and Eliav *et al.* [17]. It is clear that our CCSD(T) results are more accurate than the other two calculations. The contribution from partial triples to IP's is about 4% to 5% and it is the major reason for the high accuracy of our calculations. Comparisons with Eliav *et al.* with no triples and our calculations with triples, suggest that the omitted triples will have less than 0.1% error in the computation of IP's and EE's. The choice of our orbital basis has also contributed to the accuracy of our calculations. By representing the core, valence, and the appropriate virtual single-particle states by numerical DF/ V^{N-1} orbitals, we have been able to obtain the best physical description for them. The average error in our IP's is about 0.1% except $5d_{3/2}$, which is 0.23%. The EE's also show the same trend, the average error is about 0.6%; most of them being below 0.7%, except $6s-5d_{3/2}$, which is 1.4%. Eliav *et al.* have used the uncontracted well-tempered basis set of Huzinaga and Klobukowski [19] with 1 up to 5. Only virtual orbitals below 100 a.u. and core orbitals with $n=4$ and above, were considered for this calculation.

In the calculation by Guet and Johnson using the relativistic MBPT to second order, the IP's were computed to an accuracy of less than 2% and EE's around 4%. The accuracy of their $6s-5d_{3/2}$ excitation energy calculation is somewhat misleading, as it is a consequence of the cancellation of the errors of their $6s$ and $5d_{3/2}$ IP's. The accuracies of their $6s$ and $5d_{3/2}$ IP's are 1.5% and 1.8%. The corresponding values for Eliav *et al.* are 0.23% and 0.28% and our calculations are 0.14% and 0.23%.

By way of conclusion, we would like to state that the present paper, which is based on the relativistic coupled-cluster theory with single, double, and partial triple excitations using an orbital basis that is motivated by physical

TABLE IV. Nonlinear CCSD values for EE's in units of (a.u.).

Orbital	Experiment	Present	Eliav <i>et al.</i> [17]	Guet and Johnson [18]
$6s(1/2)-5d(3/2)$	0.022 21	0.021 91	0.024 00	0.021 36
$6s(1/2)-5d(5/2)$	0.025 86	0.026 03	0.027 76	0.025 61
$6s(1/2)-6p(1/2)$	0.092 30	0.092 46	0.092 93	0.095 66
$6s(1/2)-6p(3/2)$	0.100 02	0.100 33	0.100 71	0.103 62

considerations, is an important milestone in our quest to achieve a high-precision calculation of Ba^+ PNC.

We thank Professor Norval Fortson for useful discussions. We would like to thank C. D. A. C. Pune for providing us with the opportunity to run the codes in PARAM 10000 su-

percomputer. We thank Dr. Sundarajan and Ravinder Pal for the support. The major part of the work was done at IIA using the new E450 Sun Ultra SPARC machine with 4 CPU's and 4GB RAM. We also acknowledge the financial support from the Department of Atomic Energy (Grant No. 37/15/97-R&D.11 1603).

-
- [1] W. J. Marciano and J. L. Rosner, *Phys. Rev. Lett.* **65**, 2963 (1990).
- [2] S. C. Bennett and C. E. Wieman, *Phys. Rev. Lett.* **82**, 2484 (1999).
- [3] N. Fortson, *Phys. Rev. Lett.* **70**, 2383 (1993).
- [4] K. P. Geetha, Angom Dilip Singh, B. P. Das, and C. S. Unnikrishnan, *Phys. Rev. A* **58**, R16 (1998).
- [5] Swati Malhotra, Angom D. Singh, and B. P. Das, *Phys. Rev. A* **51**, R2665 (1995).
- [6] G. E. Brown and D. G. Ravenhall, *Proc. R. Soc. London, Ser. A* **208**, 552 (1951).
- [7] J. Sucher, *Phys. Rev. A* **22**, 348 (1980).
- [8] Z. W. Liu and H. P. Kelly, *Phys. Rev. A* **43**, 3305 (1991).
- [9] R. K. Chaudhuri, H. Merlitz, P. K. Panda, B. P. Das, Uttam Sinha Mahapatra, and D. Mukherjee, *J. Phys. B* (to be published).
- [10] I. Lindgren and J. Morrison, *Atomic Many-Body Theory*, 2nd ed. (Springer-Verlag, Berlin, 1986)
- [11] Ajay K. Mohanty and E. Clementi, *Chem. Phys. Lett.* **157**, 348 (1989).
- [12] R. K. Chaudhuri, P. K. Panda, and B. P. Das, *Phys. Rev. A* **59**, 1187 (1999).
- [13] O. Matsuoka, M. Klobukowski, and S. Huzinaga, *Chem. Phys. Lett.* **113**, 395 (1985).
- [14] O. Matsuoka and S. Huzinaga, *Chem. Phys. Lett.* **140**, 567 (1987).
- [15] O. Matsuoka and S. Okada, *Chem. Phys. Lett.* **155**, 547 (1989).
- [16] F. A. Parpia, C. F. Fischer, and I. P. Grant (unpublished).
- [17] E. Eliav, U. Kaldor, and Y. Ishikawa, *Phys. Rev. A* **53**, 3050 (1998).
- [18] C. Guet and W. R. Johnson, *Phys. Rev. A* **44**, 1531 (1991).
- [19] S. Huzinaga and M. Klobukowski, *Chem. Phys. Lett.* **212**, 260 (1993).